Rakenteiden Mekaniikka (Journal of Structural Mechanics)
Vol. 44, No 1, 2011, pp. 1-20

The effect of foundation on fan vibration response

Niko Leso, Jari Puttonen and Esa Porkka

Summary. The effect of machine frame structure or foundation on shaft vibration behavior is not always taken into account in machine design. This article investigates how different foundation alternatives affect the vibration response of the machine and evaluates the importance of modeling accuracy of the interaction between the machine and foundation. The scope of the study was a midsized fan, which is situated in an industrial environment. Foundations with different stiffness properties were analyzed both numerically and experimentally in this study. Experimental tests and calculations were performed to investigate the effect of the foundation on the fan vibration response within its assumed operational range of 30...90 Hz and with every installation alternative. MAC -values describing the modeling compatibility were calculated between measured and modeled forced vibration modes.

Key words: machine, foundation, vibration response, interaction, modeling accuracy

Introduction

The know-how of mechanical, structural and electrical engineers are combined in machine design. The design of small and midsize machines which include rotating parts are usually done in two phases: design of power transmission system and design of static structures of the machine. The effect of static frame structures or a foundation on shaft vibration behavior is not always taken into account in machine design. This in turn causes the industry interface to be also the design interface.

In this study a third phase was added to the machine design process, which accounted for the effect of foundation on shaft vibration behavior. By taking the foundation effects into account already in the machine design phase, a successful control of the whole design process can be achieved. This enables problem recognition and solving at an early stage, which reduces unexpected costs for the supplier and the customer. Considering the effects of foundation can also have concrete effect on machine operation by improving the duration of machine parts and the frame structure and also by increasing operation time of the machine.

This study investigated how different foundation alternatives affect the vibration response of the machine and evaluated the importance of modeling accuracy of the machine and foundation interaction. The study was restricted to a midsized centrifugal fan, which is situated in an industrial environment. The rotating parts of the fan were supported by ball bearings. Foundation alternatives were selected so that the stiffness ratio between the foundation and the machine differed. As a result the sensitivity of interaction phenomena for relative stiffness properties between the foundation and the different parts of the machine could be assessed comprehensively. Experimental tests

and calculations were performed to investigate the foundation effect on the vibration response of the fan in its assumed operational range of 30...90 Hz and with every mounting alternative. The dynamic excitation applied was the rotor imbalance. MAC - values describing the modeling compatibility were calculated between measured and modeled forced vibration modes.

In designing shaft vibration properties the starting point is determining the shaft natural frequencies as a free body. The support stiffness is a controlling parameter, which can be used to affect the natural frequencies of the shaft. The aim of machine shaft design is to plan the shaft natural frequencies so that they differ from the operational frequency range of the machine.

Besides the shaft itself, the shaft support and machine frame structure together affect the shaft vibration response and its location in the frequency range, but also the machine support, for example assembly frame, and its foundation affect the shaft vibration response. As a result the natural frequencies of the foundation in the machine operational range may disturb the operation and should be covered in the machine design.

Concerning machine operation, the shaft mass imbalance or rotor blade frequencies can cause problems, which occur as high vibration values. This relates specifically to resonance situations, where only the amount of damping affects the value of maximum response.

This study concentrated on investigating horizontal shafts, which can be divided into different size classes in respect of the machine and foundation interaction according to shaft mass. A machine can be classified as a small machine if the shaft mass is less than 1 % of the machine total mass. In which case, there is no need to investigate machine and foundation interaction during machine design [3]. In the case of mid size machines, the shaft mass is more than 1 %. The length of the shaft train is also an important parameter. Typical length for the shaft train of midsized industrial machines varies from 1 to 10 m.

The dynamic amplification factor

When a continuous excitation affects the system, the vibration of the system is called forced vibration. The equation of motion for the one degree of freedom vibration system with viscose damping is

$$m\ddot{x} + c\dot{x} + kx = p_0 \sin \omega t, \tag{1}$$

where m is the system mass [kg], c is the damping coefficient [Ns/m], k is the system spring or stiffness coefficient [N/m], p_0 is the excitation amplitude [N] and ω is the angular velocity of the excitation [rad/s].

The complete solution of the equation (1) is formed by two parts. The homogeneous or complementary solution represents natural oscillation, which usually damps quickly and becomes insignificant. The particular solution represents the forced vibration of the system caused by the forced excitation, which is usually dominant in a continuously operating machine.

Since the interest is in the vibrations in a stationary state, attention is generally paid to the particular solution of the equation of motion. The general solution of the equation (1) can be defined as

$$x(t) = [A\cos\omega_d t + B\sin\omega_d t]e^{-\zeta\omega_n t} + \frac{p_0}{k}\left[\frac{1}{\left(1-\beta^2\right)^2 + (2\zeta\beta)^2}\right]\left[\left(1-\beta^2\right)\sin\omega t - 2\zeta\beta\cos\omega t\right], \quad (2)$$

where A and B are coefficients defined by the initial conditions and relate to the homogeneous part, ω_d is the damped natural frequency, ζ is the critical damping ratio and β is the ratio between the excitation and the system natural frequencies.

The dynamic amplification factor describes the amplification caused by the dynamic load compared to the response caused by the static load, whose magnitude is the amplitude of the dynamic load. According to the general solution of the equation of motion (2), the amplification factor is

$$V = \frac{1}{\left(1-\beta^2\right)^2 + (2\zeta\beta)^2}, \quad (3)$$

and the phase angle between the force and motion is

$$\theta = \tan^{-1}\left(\frac{2\zeta\beta}{1-\beta^2}\right). \quad (4)$$

Figure 1 shows the dependency of the amplification factor and the phase difference as a function of the frequency and damping ratio.

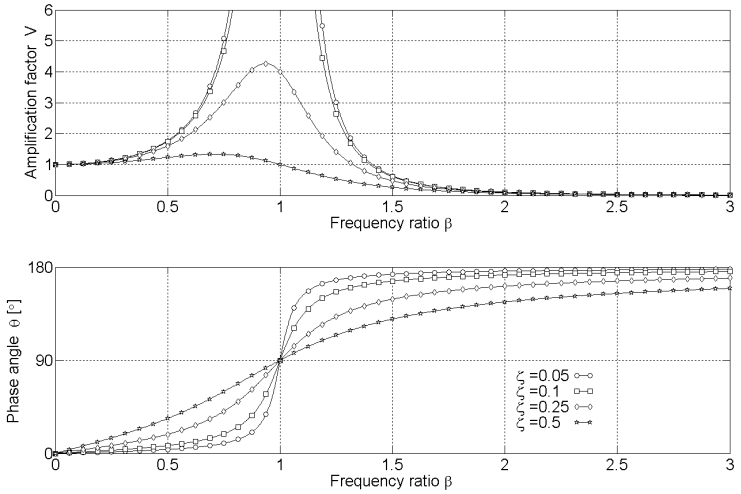

Figure 1. The amplification factor V and the phase angle θ as a function of the frequency ratio β.

The amplification factor is close to 1 when the excitation frequency is low in relation to the natural frequency of the system and the loading can be viewed as static. When the values of the frequency ratio are high, the values of the factor V approach zero asymptotically. In other words, a high frequency excitation comparable to the system natural frequency does not affect a significant displacement response to the system, but according to the vibration equation the outside load is balanced by the acceleration of the system mass.

In resonance the frequency ratio β is 1, in which case the vibration amplitude reaches its maximum value and the amplification factor is $1/2\zeta$. Only the damping ratio limits the value of the amplification factor in resonance or in its vicinity. The phase angle θ is 90° in resonance and 180° with high values of the frequency ratio. With high values of the damping ratio, the amplification factor does not achieve significant gain. Respectively, the value of the amplification factor grows substantially with low values of the damping ratio. In the resonance of the undamped system, the amplification factor and also the system displacement grow infinitely large in theory. This is why the effect of damping is significant especially in the system resonance areas.

System vibration response in the frequency domain

Introduction

The general solution of the vibration equation defines the vibration in the time domain. The solved vibration response of the system corresponds only to a specific value of the excitation frequency. The Fourier transform of the equation of motion leads to a static equation, which enables the vibration of the system to be described in a specific frequency range. The achieved result is usually called a frequency domain solution. The frequency domain solution contains the needed information about the forced vibration of the system under an excitation force in a specific frequency range.

Solution in the frequency domain

Applying the Fourier transform to the equation of motion (1), the equation obtained for the displacement in the frequency domain is

$$X(\omega) = H(\omega)F(\omega), \tag{5}$$

where $X(\omega)$ is the Fourier transform of the response, $H(\omega)$ is the frequency response function of the examined system and $F(\omega)$ is the frequency response function of the excitation. The equation (5) is applied e.g. in vibration tests, where measurement signals of the excitation and response of the examined system are stored in time domain with a measuring instrument. The stored measurement signals are Fourier transformed using the measuring instrument or a separate computer program. After this the examined frequency transfer function $H(\omega)$ can be solved using the following equation

$$H(\omega) = \frac{X(\omega)}{F(\omega)}. \tag{6}$$

The Fourier transform of the equation (1) can be defined as

$$(-\omega^2 m + i\omega c + k)X(\omega) = F(\omega), \tag{7}$$

when the frequency transfer function $H(\omega)$ of equation (6) is given by

$$H(\omega) = \frac{1}{-\omega^2 m + i\omega c + k} = \frac{1}{k} \cdot \frac{1}{(1-\beta) + i(2\zeta\beta)}. \tag{8}$$

Dynamic stiffness is given as an inverse of the frequency transfer function. Generally the results of dynamic measurements are viewed in the frequency domain, especially when dealing with long term dynamic excitations.

Research objects

The fan

The fan used in the research has been presented in figure 2. The mass of the rotor was 160 kg and the total mass of the machine was 2405 kg. The width and length of the fan were 0.96 and 2.39 m.

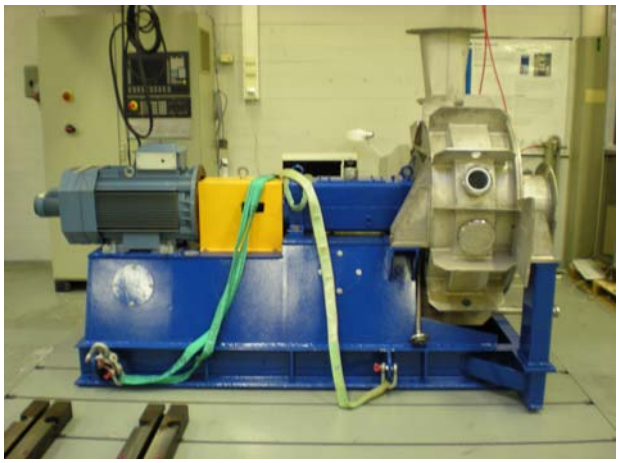

Figure 2. The centrifugal fan used in the study.

The fan is designed for different industrial processes to recycle gas or air of wide heat fluctuations. The fan operation is based on exceeding the pressure loss of the system with a counter pressure formed by the rotor. This causes airflow between the inlet and outlet openings of the fan.

The foundation alternatives

Test facility K3 is part of the Department of Engineering Design and Production at Aalto University School of Engineering. The facility width is 12 m, length 28 m and height 5 m. The height of the ground floor under the slab structures is 2.75 m. The load

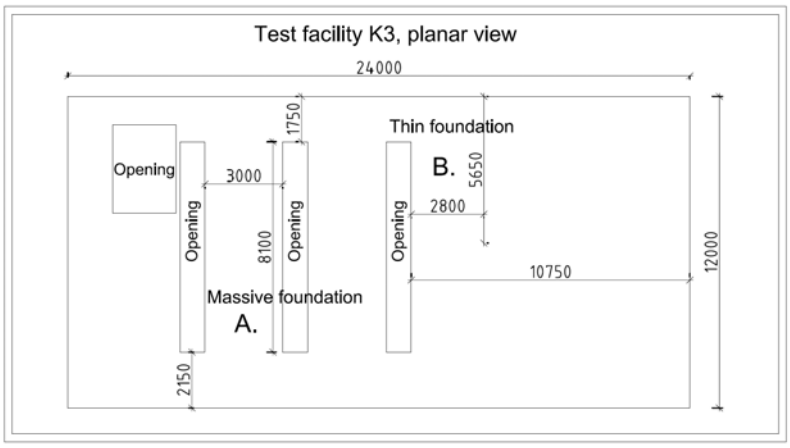

Figure 3. A planar view of test facility K3 structures.

bearing structures are columns and beams. Figure 3 shows a planar view of structures around the locations A and B of the fan. The modeling of the foundation structures covered the area presented in the figure.

The test facility K3 column grid spacing is 4 m lengthwise and 6 m widthwise. The slab is supported by column, beam and wall structures. The columns are founded using piled column footings and the wall structures rest on a soil-supported ground slab.

Two mounting alternatives were used to describe a massive stiff foundation (mounting situation A) and a thin or flexible foundation (mounting situations B1 and B2). The massive foundation had a slab thickness of 750 mm and it was supported rigidly by two massive wall elements connected to the ground slab. The thin foundation had a slab thickness of 250 mm. The table slab of the thin foundation was continuous and it was supported on all sides by wall elements.

The frequency response functions (6) of the foundation alternatives were determined from shock measurement results and the dominant natural frequencies of the massive and thin foundation were 155 and 70 Hz. The dynamic stiffness of the massive foundation was 5.0×10^9 N/m at a frequency of 50 Hz, when it was 2.0×10^8 N/m in the case of the thin foundation. Thus dynamic properties of the selected foundations were clearly different.

The fan mounting

In the mounting situation A the fan was mounted with rail beams and steel bolts and in the mounting situation B1 by using steel bolts. The objective was to make the mounting as rigid as possible, so that the foundation effect to the machine dynamic behavior would be as clear as possible. A target in the machine installation was to guarantee that the support reactions created by the mounting would be known as precisely as possible. This was done by limiting the contact surface between the fan and the foundation only to the areas of the mounting points. The connection between the machine and foundation was assumed to be rigid at the coverage areas of the mounting points.

In the mounting situation B2 the fan was mounted using six rubber isolators. The location of the fan corresponded with the mounting situation B1. In the study the rubber

isolators were tested and according to results a single rubber isolator had a linear loading/deflection graph with a static stiffness of 7.1×10^5 N/m, which was close to the value of the design table of the isolator. The isolators were modeled using axial struts, which had the same value of stiffness as the testing result and the same height as the isolators.

The fan and foundation modeling

Introduction

A calculation model of the fan and the foundation structures was created using SIMULIA Abaqus® 6.8 software, which is based on the finite element method. The modeling process was completed in different phases, which included the static part and the shaft of the fan and the structures of the different foundation alternatives. In the study the element models of the fan and foundation structures were done according to existing structures and therefore were highly accurate compared to the typical practical design situation.

The fan`s static part

The fan static part (Figure 4) consists of a frame structure, an impeller shell structure, a bearing housing and also in this case an electric motor. The parts of the fan assembly are made of different steel grades. The parts were modeled as homogeneous material with Young's modulus 210 GPa, Poisson's ratio 0.3 and mass density 7850 kg/m ^{3}. The frame structure was modeled using shell elements and it forms the support for the bearing housing, the electric motor and the impeller shell structure. The bearing supports were modeled using solid elements. The electric motor is attached to the shaft via a shaft coupling and it was also modeled using solid elements. The structures of the static part are welded or bolted together, so the structural connections were modeled as rigid joints.

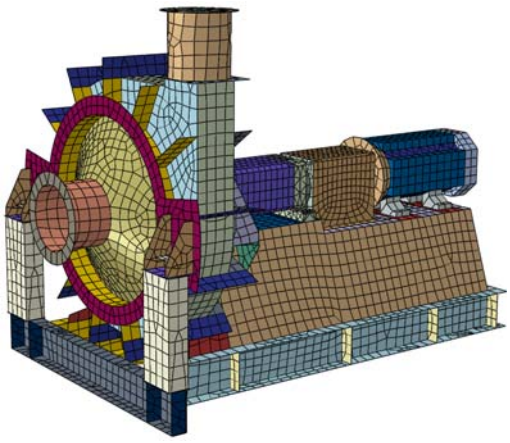

Figure 4. The finite element model of the static parts of the fan.

The finite element model of the static part of the fan included approximately 12 700 elements and 49 000 degrees of freedom. The side length of the shell elements was approximately 50 mm and the characteristic length of the face of the solid elements was approximately 40 mm.

The fan`s shaft

A shaft and impeller of the fan form an entity usually called a rotor. The diameter of the impeller was 800 mm and the length of the steel shaft was 1320 mm. The impeller was modeled using shell elements and the shaft using three dimensional beam elements. The length of a single beam element was approximately 20 mm and the shaft model had a total of 79 elements. The impeller model had a total of 717 shell elements and the side length of a single element was approximately 50 mm.

The fan shaft is attached to the frame structure with two bearing supports and it is connected to the electric motor shaft via a shaft coupling. The fan bearings are roller bearings and their support in connection with the shaft was assumed to be a two way hinge. The support between the bearings and the shaft was modeled using vertical and horizontal axial struts and each strut was given a value corresponding with the bearing stiffness of 200 MN/m given by the fan supplier.

The foundation structures

The slab and their support structures (Figure 5) were modeled including the massive and thin foundation alternatives and the structures around the foundations. The surrounding structures enhanced the modeling accuracy of the dynamics of the foundation alternatives and their modeling also enabled the distribution of the vibration energy to a larger area around the machines. The test facility structures were taken into account for the width of the test facility and 24 m lengthwise.

The concrete structures were modeled as homogeneous material with Young's modulus 29.96 GPa, Poisson's ratio 0.3 and mass density 2400 kg/m ^{3}. The structures were modeled using solid elements and rigid joints between structural connections. The length and width of prism elements were approximately 200 mm and the height was approximately 125 mm. The element model of the concrete structures included approximately 66 000 elements and nodes and 171 000 degrees of freedom.

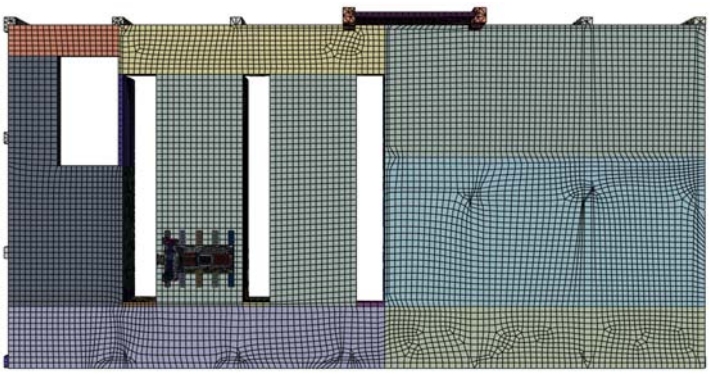

Figure 5. A planar view of the element model of the concrete structures of the test facility K3.

Boundary conditions applied to the edges corresponded with the effects of the surrounding structures. The left and right edges of the model were modeled as a rigid support, because the stiffness of the massive slab and beam structures surrounding the model were large compared to the structures around the model edges. The upper and lower edges of the model were restricted by the test facility`s wall structures and joint type boundary conditions were applied to the aforementioned edges, which describe the connection between a wall and a slab. The model was limited to the level of the ground slab and only the horizontal support reaction of the slab for the vertical structures was taken into account. Otherwise hinge boundary conditions were applied to columns and walls at the level of the ground slab.

Vibration testing during the fan operation

Introduction

The dynamic load of the fan spreads from the point of the force through the shaft support to the fan frame structure and onto the foundation. Vibration tests were performed to investigate how different foundation alternatives affect the maximum response and value of the shaft, when the fan is run up through its operational range. In tests were also investigated how foundation vibration levels changed between mounting situations by observing the responses at the mounting points of the fan. The propagation of vibration and its damping was investigated by measuring the responses of the slab at different distances from the fan.

The testing process

The aim of the vibration tests was to determine the first order vibration responses of the measurement points in a specific frequency range caused by a known 2.05 g imbalance mass. The known imbalance mass was located on the outer rim of the impeller and it corresponded to an 820 g·mm imbalance change compared to the original state of balance.

The measurements were done in every mounting situation, first in the original state of balance of the shaft and then in the state of balance, which corresponded to the original state plus the known imbalance mass. The testing results relating to the known imbalance mass were received by subtraction.

During testing the rotational speed of the fan range was 30...90 Hz and the fan was operated using constant rotating speed intervals of 1 Hz. Figure 6 shows the locations of the acceleration transducers on the fan frame structure and the distances between them. Points 1…6 relate to the mounting points of the fan from which vertical acceleration was measured. Points 7 and 8 are situated on the bearing supports from which vertical and horizontal acceleration was measured.

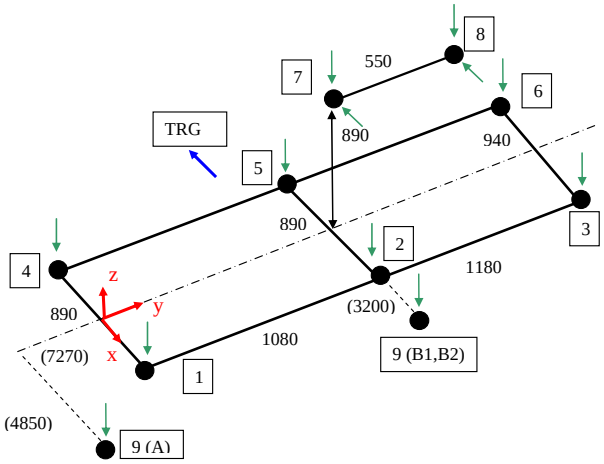

Figure 6. The locations of the acceleration transducers.

The measurement point 10 outside the fan was located on the massive foundation and its distance from the measurement point 2 was 2.9 m in the mounting situation A and 8.7 m in the mounting situations B1 and B2. In the mounting situation A the measurement point 9 was located in the middle of the thin foundation 9.5 m from the measurement point 2. In the mounting situations B1 and B2 the measurement point 9 was located in the middle of the slab next to the thin foundation 3.2 m from the measurement point 2.

The experimental vibration analysis was restricted to the harmonic components of the rotating speed of the fan from which only the first order response was taken into account. The harmonic components were analyzed using a separate analysis program within the MATLAB software. The response graphs of the measurement points in a frequency range of 30...90 Hz, relating to the known test mass, were determined using the measured vibration signals of the measurement points.

The computational response analysis

The results of the numerical response analyses correspond with the testing results, which enabled a straight forward response graph comparison. The theory used by the Abaqus software corresponds with the theory used in this study and demonstrated by the equations of the one degree of freedom systems. The software solves the system eigenvalues and the corresponding eigenvectors using the Lanczos method, which is discussed more thoroughly e.g. in reference [4]. At the measurement points vibration responses were determined using modal superposition. In this case the system vibration response to a harmonic excitation is determined based on the modes defined for an undamped system.

The radial dynamic loading caused by the imbalance of the fan was modeled using two sine shaped vibration forces. The forces were located at the center of the rotor shaft. The effect of a rotating force was created by a phase difference of 90 °. The force amplitude corresponds with the resultant force of the imbalance mass

$$p_0 = me\omega^2 , \qquad (9)$$

where *m* is the imbalance mass [kg] and *e* is the distance of the mass from the axis of the rotating shaft [m]. The fan and foundations damping was introduced by a critical damping ratio and a constant value of damping was set at the specified frequency range. The value of the damping ratio was 2 % at each mounting situation, which is also the value recommended by the standard DIN 4024 [3].

The results of computational response analyses

The fan natural modes

The natural modes of the fan shown in the response analysis results (Figure 7) are interpreted visually. In the element model the bending mode of the rotor is not purely vertical or horizontal because the stiffness of the rotor support structures is different in the horizontal and vertical directions. The front section of the fan describes the vibration motion of the impeller shell and its support structures, which corresponds without exception to a rotation mode around the shell support beams. The back section covers the rest of the frame structures of the fan and its motion is almost always horizontal translation vibration.

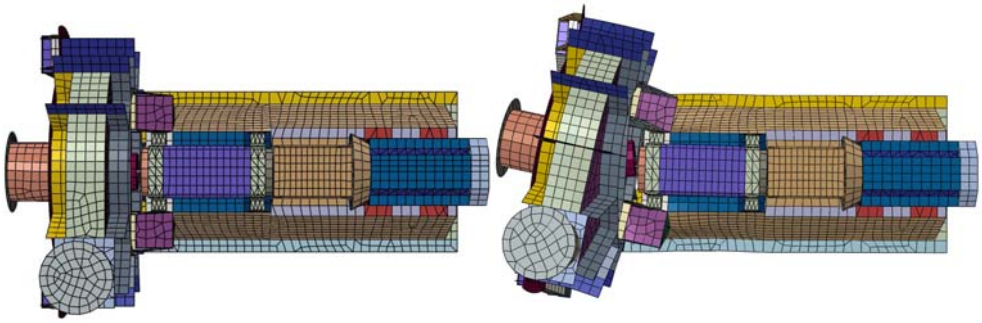

Figure 7. The undeformed (left) state of the fan and the end vibration motion (right) of the most common fan natural mode.

The response analysis result comparison

The vibration levels calculated for the fan mounting points and shaft were done using measurement points 3 (Figure 8) and 7z (Figure 9). The response graphs of the measurement points have been shown in the specific frequency range and in every mounting situation. In this case the natural frequencies of the shaft were in practice identical between the different mounting situations.

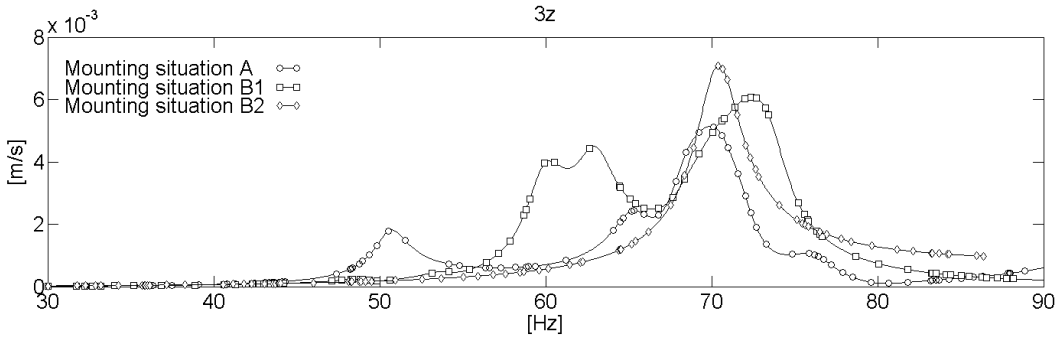

Figure 8. Comparison of calculated velocity responses at point 3.

Only one resonance peak exists in the mounting situation B2 and the peak response in relation to velocity is ±7.1 mm/s. The mounting with isolators is a separate case and only the mounting situations A and B1 describe the effect of the massive and thin concrete foundation. In the case of the massive foundation the maximum response of the mounting points is ±5.2 mm/s and in the case of the thin foundation ±6.1 mm/s. The vibration levels at the mounting points and also at the foundation are close to each other irrespective of the foundation alternative.

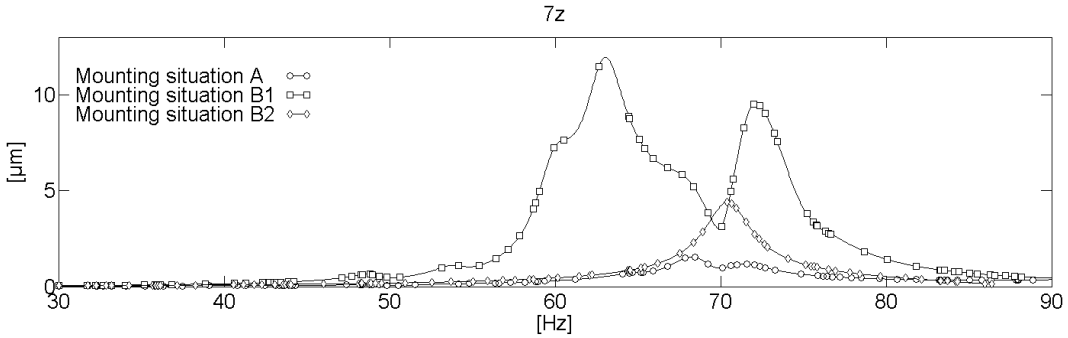

Figure 9. Comparison of calculated displacement responses at point 7z.

In the mounting situations A and B1 the measurement point 7z has the maximum response peaks at frequencies 68 and 63 Hz and their amplitudes are 1.6 and 12.0 µm. In the case of the thin foundation the shaft response is 7-fold compared to the massive foundation. In the mounting situation B1 the vibration of the foundation is clearly associated to natural frequencies of the fan. As a result the effect of the foundation on the vibration behavior of the fan is significant in mounting situation B1. In the mounting situation B2 the maximum response resonance peak is located at frequency 70 Hz and its amplitude is 4.4 µm.

Vibration test result comparison

The aim was to evaluate how mounting and foundation alternatives affect the vibration response of the fan in reality. Measurement points 3 (Figure 10) and 7z (Figure 11) were

selected to the comparison. The response graphs of the measurement points have been shown in the specific frequency range and in every mounting situation

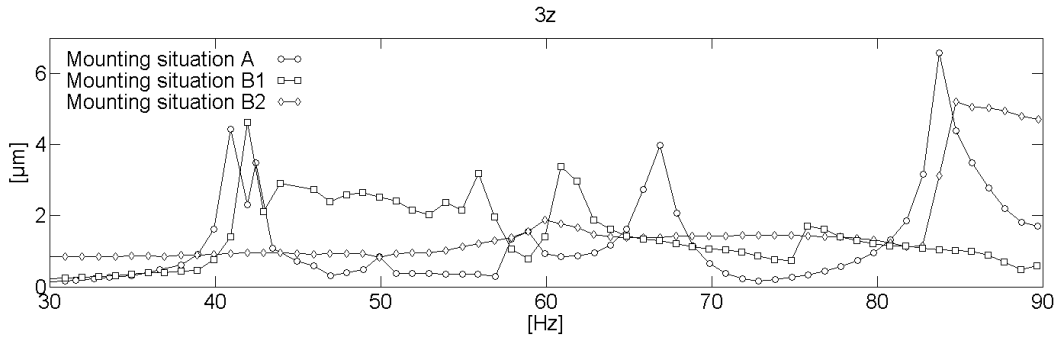

Figure 10. Comparison of measured displacement responses at point 3.

Only one resonance peak with a response of ±5.3 µm exists in the mounting situation B2 (Figure 10). The mounting situations A and B1 describe the effect of the massive and thin foundation. In the mounting situation A, the resonance peaks corresponding to the natural modes are distinctive, whereas in the mounting situation B1 the response is distributed along a wide frequency range. Because of the complex dynamics associated with the thin foundation, the dynamic excitation is divided among several different natural modes. In the case of the massive and thin foundation, the maximum mounting point responses are ±6.7 and ±4.8 µm at 84 Hz and 42 Hz, respectively.

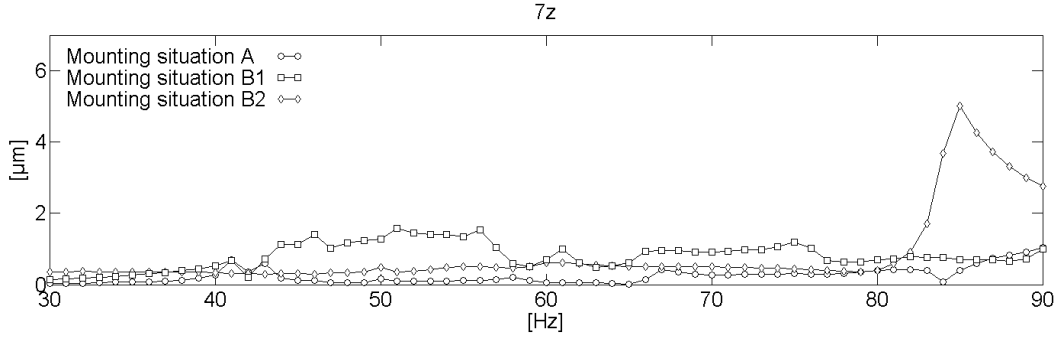

Figure 11. Comparison of measured displacement responses at point 7z.

Only one resonance peak with a response of ±5.0 µm exists in the mounting situation B2 (Figure 11). The use of the isolators enables much higher vibration responses compared to mounting situations A and B2. In the mounting situations A and B1, the maximum responses of measurement point 7z are ±0.6 and ±1.6 µm at 41 Hz and 56 Hz respectively. In the case of the thin foundation the vibration response is approximately 3-fold compared the massive foundation in a frequency range of 43…85 Hz.

Table 1. The calculated and measured maximum response amplitudes and their frequencies at points 3, 7z and 7x in every mounting situation.

Mounting situation A	Measured response [Hz/µm]	Calculated response [Hz/µm]
3	84/6,7	76/11,7
7z	90/1	68/1,6
7x	41/16	51/8,8
Mounting situation B1		
3	42/4,8	63/11,4
7z	56/1,6	63/12
7x	42/14,9	60/4,6
Mounting situation B2		
3	84/5,3	70/16
7z	84/5,0	70/4,4
7x	84/5,0	70/1,4

Calculated and measured response comparison

Table 1 shows the calculated and measured maximum response amplitudes and their frequencies at points 3, 7z and 7x in every mounting situation.

In the mounting situation A, the differences between the test and calculation results in horizontal responses were caused by the modeled horizontal stiffness, which was higher than the actual situation. This can be seen from the maximum response values of measurement point 7x in every mounting situation. The horizontal stiffness of the bearing unit is lower than the rigid joint used in the model.

In the mounting situation B1 the calculated vertical maximum response of the back bearing was almost 8-fold compared to the measured value. The actual stiffness of the mounting does not match with the modeled ideal situation, which leads to differences in maximum responses. The modeled rigid mounting enables clear combined fan and foundation natural modes. The actual mounting stiffness is lower, so the vibration motion of the fan and foundation is not completely uniform.

In the mounting situation B2 the low isolator stiffness and the flexible fan mounting isolated the fan from the environment. In this case the mounting and foundation do not affect the fan dynamics or participate in its operation. The differences between the measured and modeled responses result likely from inaccurate modeling of the isolator properties. The isolator modeling was done using only vertical static stiffness. Determination of the dynamic frequency dependent isolator stiffness was neither possible during this study.

Vibration propagation

In the mounting situation A the measured maximum amplitude at the measurement point 9 (Figure 6) was 0.24 µm and the corresponding calculated result was 0.82 µm. In the model the resonance peak related to a joint natural mode of the fan and foundation structures. According to the test results, it is not certain that that the maximum response corresponds to a joint natural mode or if it is a case of geometric damping, which decreases the vibration as a function of distance from the point of excitation.

In the mounting situation B1 the measured maximum amplitude at the measurement point 9 was 1.5 µm and the corresponding calculated result was 3.9 µm. According to maximum response values in the mounting situations A and B1 the modeled value of the measurement point 9 is almost 3-fold compared to the measured value. This is probably a result of inaccurate damping value of the foundation structures or structural discontinuities.

One of the objectives to use isolators was to verify that the vibration resulting from the operation of the fan does not propagate to the structures outside the fan. In the mounting situation B2 the measured and calculated vibration response maximum amplitude of the measurement point 9 was approximately a hundredth of micrometer. This confirmed that the rubber isolators efficiently isolated the vibration propagation.

Modal analysis using peak picking

In the modal analysis, the natural modes of the fan were determined according to the highest resonance peaks of the measured and calculated response graphs in every mounting situation. First the highest resonance peaks were selected from those response graphs, which included the highest number of distinct response peaks. The locations of the selected resonance peaks in the frequency domain correspond to the modal frequency of the fan. Next the real and imaginary parts of the vibration corresponding to the selected resonance peak frequencies were determined. The vibration motion of a certain measurement point can be described as a whole by using these two parts. The modal analysis was performed using a separate analysis program within the MatLab software according to the mode specific real and imaginary parts. As a result the measured and calculated forced vibration modes of the fan were determined in every mounting situation. The vibration motion of the measurement points was described with amplitude and phase shift.

MAC-criterion

MAC (Modal Assurance Method) [1, 5] enables a congruity comparison of two mode vector groups describing a vibration motion. The comparison can be made between a measured and modeled, two measures or two modeled natural modes. The MAC-criterion is used to solve the correlation factor between two natural modes. An element of the MAC-matrix for a mode vector pair is given by

$$MAC\left(\{\varphi_A\}_j, \{\varphi_B\}_k\right) = \frac{\left|\{\varphi_A\}_j^T \{\varphi_B\}_k\right|^2}{\{\varphi_A\}_j^T \{\varphi_A\}_j \{\varphi_B\}_k^T \{\varphi_B\}_k}, \quad (10)$$

where $\{\varphi_A\}_j$ is the j:th mode of the mode vector group $A_{n\times m}$, $\{\varphi_B\}_k$ is the k:th mode of the mode vector group $B_{n\times m}$, m is the number of the mode vectors and n is the number of the mode vector elements. The MAC-matrix elements receive a value between zero and one and they are always real regardless if the modes are real or complex. The method gives a value of one if the natural modes match each other completely and a value of zero if the modes do not correlate at all. In practice the modes can be considered identical if the MAC-value is higher than 0.90 and completely different if the value is 0.05 or less [2].

Mode-specific comparison

The mode-specific comparison was done using the MAC-criterion between the measured and modeled natural modes of the fan in every mounting situation. The mode vector group consisted of complex valued mode vectors corresponding with the measurement points, which were determined in context with the modal analysis using peak picking. The MAC-criterion does not take the natural mode frequencies into account.

In total of 10 natural modes of the fan were determined according to test results and in total of 7 natural modes were determined according to modeling results. Table 2 shows the numbering and frequencies of the measured and modeled fan natural modes in every mounting situation.

Table 2. The numbering and frequencies of the measured and modeled fan natural modes.

	Measured [nr./Hz]	Modeled [nr./Hz]
Mounting situation A	1/42	1/51
	2/57	2/65
	3/67	3/71
	4/84	
Mounting situation B1	5/42	4/60
	6/57	5/63
	7/67	6/72
	8/84	
	9/89	
Mounting situation B2	10/84	7/71

Table 3. The MAC-values for fan natural modes in the mounting situation A.

Measured [nr.]	Modeled [nr.]	MAC-value [%]
1	1	96
2	2	43
3	3	80

Table 4. The MAC-values for fan natural modes in the mounting situation B1.

Measured [nr.]	Modeled [nr.]	MAC-value [%]
6	5	44
6	6	44
7	4	50
7	6	39

Mounting situation A

Table 3 shows the most accurate MAC-values between the measured and modeled mode vector groups in the mounting situation A.

It can be seen from the MAC-values that the modeled natural mode 1 corresponds exactly to the measured mode 1. The modeling accuracy of frequency between the modes is 82 %. The modeled natural mode 3 correlates the most with the measured mode 3 and the modeling accuracy of frequency is 94 %. It can be concluded from the above values that in the mounting situation A the modeled natural modes correspond fairly well to the actual situation on behalf of the geometric shape and frequency of the vibration motion. Only the damping value affects the magnitude of the vibration response. In the element model the relative damping was 2 % in the specific frequency range, which corresponded accurately to the actual damping in mounting situation A. Because of the high stiffness of the massive foundation and the low damping of the mounting, the foundation effect on the dynamic operation of the fan was insignificant. As a result, good accuracy can be achieved in the modeling of the machine natural modes if the machine is mounted rigidly on a high stiffness foundation.

Mounting situation B1

Table 4 shows the most accurate MAC-values between the measured and modeled mode vector groups in the mounting situation B1.

It can be seen from the MAC-criteria that the modeled natural mode 4 corresponds most accurately to the measured mode 7 and the modeling accuracy of frequency is 98 %. The modeled natural modes 5 and 6 correlate evenly to the measured mode 6 and the modeling accuracies of frequency are 70 and 93 %. It can be concluded from the

above values that in the mounting situation B1 the mode specific frequencies of the element model correspond accurately to the actual situation. In the mounting situation B1 the mode specific vibration motions correspond with the geometry of the measured natural modes more poorly compared to the situation A. The verification of the foundation element model indicated that the model of the thin foundation corresponds fairly accurately to the actual situation. The differences between the measured and modeled vibration motions are likely a result of inaccuracies in modeling the interaction between the fan and foundation alias the mounting.

Mounting situation B2

The MAC-value between the measured natural mode 10 and the modeled mode 7 was 31 %. It can be concluded from this value that the natural modes do not correlate as accurately compared to the mounting situations A and B1. The vibration motions of the measured and modeled modes corresponded fairly well each other, but the differences in the vibration amplitudes were significant. Based on the preliminary verification of the fan element model, the fan frames structure modeling corresponds to the actual situation. The differences between the amplitudes are likely a result of inaccurate modeling of the function and frequency dependency of the isolator, because the rubber isolators did isolate the fan from the environment. The frequency modeling accuracy of 85 % between the modes was fairly good.

Conclusions

The measured vertical maximum response amplitudes of the fan bearing situated on the motor side and mounting points were in situation A 1 and 6.7 µm and in the situation B1 1.6 and 4.8 µm. According to the measured fan resonance peak amplitudes, there were no significant differences concerning machine operation between the massive and thin foundation. In this case simple and relatively small excitation of the fan did not extensively excite the natural modes of the thin foundation.

The calculated and measured vertical vibrations of the fan were close to each other in the mounting situation A. In the mounting situation B1 the measured and calculated vibration responses differed significantly. In the element model the maximum amplitude at the bearing housing was 8-fold compared to the measured value. In the model the parts at the interfaces of the fan and the foundation moved in the same phase, but in reality phase differences appeared between the parts. The modeled fan mounting on the thin foundation was completely rigid, but in reality the connection was flexible, which in part decreases the values of the measured vibration responses. The above information tells about the difficulty to model the connection between the machine and foundation accurately enough in case of dynamic loads. The function of machine and foundation connection can be estimated by experimentally defining how flexible the connection is and which of the structures forming the connection are the most flexible during dynamic loading. These frequency dependent flexibility values can be used in the modeling of these interfaces.

The MAC-criterion describing the compatibility between measured and modeled forced vibration modes were determined according to the modal analysis using peak picking in every mounting situation. On the massive foundation, the calculated natural mode compatibilities of the fan in relation to measured values were 43 - 96 % and the frequency compatibilities were 82 - 94 %. In the mounting situation A, the modeled natural modes correspond fairly well to the actual situation as far as the geometric shape and frequency of the vibrations are concerned. As a result of the simple dynamics of the massive foundation in the operational range of the fan and high natural frequencies, the effect of the foundation on the dynamic behavior of the fan was insignificant. In practice, a machine mounted on a foundation with stiffness clearly higher than the machine frame structure, gives a good modeling certainty.

In the mounting situation B1, the calculated compatibilities of natural modes in relation to measured values was 39 - 50 % and the frequency compatibility was 70 - 98 %. On the thin foundation, the mode specific vibration motions corresponded to the measured natural modes more poorly compared to the mounting situation A, but the mode specific frequencies corresponded to the actual situation. The dynamics of the thin foundation were complex compared to the massive foundation at the operational range studied. As a result, the simple and relatively small excitation of the fan was not likely to be able to excite all of the thin foundations natural modes. This affected the certainty of mode specific comparison between the measured and modeled modes, because it may be possible that a part of the calculated natural modes included in the comparison did not appear in the measurement results. The amplitude and phase angle differences between the measured and modeled vibration motions were especially a result of inaccuracies in the modeling of the fan and foundation interaction. It can be recommended that the machines of the type investigated are useful to mount on (e.g. rubber) isolators if the foundation is flexible. In this case by using the isolators the effect of the foundation can mostly be disregarded in evaluation of the behavior of the machine.

In the mounting situation B2, the calculated compatibility of natural modes in relation to measured value was 31 % and the frequency compatibility was 85 %. When the fan was mounted with rubber isolators, the modes of the fan did not correlate as accurately compared to the mounting situations A and B1 and especially the mode specific vibration motion amplitudes differed. This was likely a result of inaccuracy in the modeling of the isolators as the modeling of the fan frame structure corresponds to the actual situation and the rubber isolators isolated the fan from the environment. According to available background information, the isolators were modeled using static stiffness, which is based on the loading caused by the mass resting on the isolators. The modeling of the rubber isolators may be necessary to be based on dynamic stiffness values.

The evaluation of the modeling accuracy using MAC-criteria can be improved by determining the measured and calculated forced vibration modes of the structure as accurately as possible. It is important to have a high number of measurement points and directions and to locate the measurement points to dominant areas of the vibration motion, so that the measured modes would be as accurate as possible. At the same time the frequency resolution should be sufficient. In this study, the frequency resolution was

1 Hz in vibration tests. As a result it is possible that the frequency domain connection between measured forced vibration and natural frequencies of the fan could not be done accurately enough.

The phase shifts corresponding to the resonance peaks of the calculated response graphs were in certain cases close to 180 ° within a very narrow frequency range. The forced vibration modes determined according to resonance peaks in question can change if the phase angle values are not selected precisely at the frequency of the resonance peak location. This can affect significantly the value of MAC-criterion describing the compatibility of the measured and calculated forced vibration modes.

From the practical point of view it should be considered that in this study the fan and foundation structures were modeled based on existing structures and construction and manufacturing drawings. Therefore the modeling was fairly accurate compared to the design situations in practical projects, where these types of fans or machine are used. The results presented in this article may also give an idea of the accuracy or inaccuracy of the practical design calculations in that kind of applications.

References

[1] Allemang R. J, Brown D. L, A Correlation Coefficient for Modal Vector Analysis, 1st International Modal Analysis Conference 1982, Nov. 8-10, 1982, Orlando.

[2] Avitable P, O´Callahan P, Milani J, Model correlation and orthogonality criteria, 6th International Modal Analysis Conference 1988, Feb. 1 - 4, 1988, Kissimmee.

[3] DIN 4024-1.1988, Machine foundations; Flexible Structures that Support Machines with Rotating Elements, Deutsches Institut Für Normung E.V, Germany.

[4] Ericsson T, Ruhe A, The Spectral Transformation Lanczos Method for the Numerical Solution of Large Sparse Generalized Symmetric Eigenvalue Problems, *Mathematics of Computation*, 1980.

[5] Ewins D. J, *Modal Testing: Theory and Practice*, Research Studies Press Ltd, Hertfordshire 1986.

Niko Leso, Jari Puttonen, Esa Porkka
Aalto University School of Engineering
P.O. Box 11000, FIN-00076 Aalto, Finland
niko.leso@tkk.fi, jari.puttonen@tkk.fi, esa.porkka@tkk.fi